ANTIOXIDANTS & REDOX SIGNALING
Volume 15, Number 10, 2011

DOI: 10.1089/ars.2011.4065

The Crucial Role of Early Mitochondrial Injury in L-Lysine-Induced Acute Pancreatitis

György Biczó,[1] Péter Hegyi,[1] Sándor Dósa,[2] Natalia Shalbuyeva,[3] Sándor Berczi,[2] Riitta Sinervirta,[4] Zsuzsanna Hracskó,[5] Andrea Siska,[6] Zoltán Kukor,[7] Katalin Jármay,[1] Viktória Venglovecz,[8] Ilona S. Varga,[5] Béla Iványi,[2] Leena Alhonen,[4] Tibor Wittmann,[1] Anna Gukovskaya,[3] Tamás Takács,[1] and Zoltán Rakonczay, Jr.[1]

Abstract

Aims: Large doses of intraperitoneally injected basic amino acids, L-arginine, or L-ornithine, induce acute pancreatitis in rodents, although the mechanisms mediating pancreatic toxicity remain unknown. Another basic amino acid, L-lysine, was also shown to cause pancreatic acinar cell injury. The aim of the study was to get insight into the mechanisms through which L-lysine damages the rat exocrine pancreas, in particular to characterize the kinetics of L-lysine-induced mitochondrial injury, as well as the pathologic responses (including alteration of antioxidant systems) characteristic of acute pancreatitis. ***Results:*** We showed that intraperitoneal administration of 2 g/kg L-lysine induced severe acute necrotizing pancreatitis. L-lysine administration caused early pancreatic mitochondrial damage that preceded the activation of trypsinogen and the proinflammatory transcription factor nuclear factor-κB (NF-κB), which are commonly thought to play an important role in the development of acute pancreatitis. Our data demonstrate that L-lysine impairs adenosine triphosphate synthase activity of isolated pancreatic, but not liver, mitochondria. ***Innovation and Conclusion:*** Taken together, early mitochondrial injury caused by large doses of L-lysine may lead to the development of acute pancreatitis independently of pancreatic trypsinogen and NF-κB activation. *Antioxid. Redox Signal*. 15, 2669–2681.

Introduction

Despite intensive research, the pathogenesis of acute pancreatitis is unclear, especially concerning the early events (24). Our current understanding of acute pancreatitis comes mainly from studying experimental disease models. Premature activation of trypsinogen (11, 29), the activation of the proinflammatory transcription factor nuclear factor-κB (NF-κB) (27), and mitochondrial injury (8, 22) in pancreatic acinar cells are commonly thought to play an important role in the development of acute pancreatitis. However, the sequence and relationship of these processes are matters of debate (27).

Large doses of intraperitoneally (i.p.) injected basic amino acids L-arginine or L-ornithine induce acute pancreatitis in rodents, although the mechanisms mediating the toxicity remain unknown (6, 10, 28, 31). Another basic amino acid, L-lysine, was also shown to cause acinar cell injury (14, 15). Further, a marked swelling of pancreatic mitochondria was reported in L-lysine-treated rats. Here we performed a detailed

Innovation

We have demonstrated that large doses of intraperitoneally injected L-lysine induce acute necrotizing pancreatitis. L-lysine administration caused early pancreatic mitochondrial damage that preceded the activation of trypsinogen and the proinflammatory transcription factor NF-κB, which are commonly thought to play an important role in the development of acute pancreatitis. Our data suggest that early mitochondrial injury may lead to the development of acute pancreatitis.

[1]First Department of Medicine and [2]Department of Pathology, University of Szeged, Szeged, Hungary.
[3]Veterans Affairs Greater Los Angeles Healthcare System and University of California, Los Angeles, California.
[4]Biotechnology and Molecular Medicine, A.I. Virtanen Institute for Molecular Sciences, Biocenter Kuopio, University of Eastern Finland, Kuopio, Finland.
Departments of [5]Biochemistry and Molecular Biology and [6]Clinical Chemistry, University of Szeged, Szeged, Hungary.
[7]Department of Medical Chemistry, Molecular Biology, and Pathobiochemistry, Semmelweis University, Budapest, Hungary.
[8]Department of Pharmacology and Pharmacotherapy, University of Szeged, Szeged, Hungary.

investigation of the effects of L-lysine on parameters of pancreatic injury, as well as on mitochondrial function. The aim of the study was to get insight into the mechanisms through which L-lysine damages the exocrine pancreas, in particular to characterize the kinetics of L-lysine-induced mitochondrial injury, as well as the pathologic responses characteristic of acute pancreatitis.

Here we show that L-lysine induced all the typical responses of acute pancreatitis, including morphologic changes, mitochondrial damage, and activation of trypsinogen and the proinflammatory transcription factor NF-κB. We further show that mitochondrial injury occurs from a very early time point that precedes both the premature activation of trypsinogen and the activation of NF-κB. Importantly, L-lysine selectively damaged pancreatic mitochondria, without any effect on liver mitochondria.

Results

Dose response of i.p. injection of 1–5 g/kg L-lysine

The mortality rates observed in groups of rats treated with different doses of L-lysine were as follows: 0–2 g/kg, 0% ($n=6$–12); 2.5 g/kg, 43% ($n=7$); 3 g/kg, 54% ($n=13$); 3.5 g/kg, 80% ($n=5$); 4–5 g/kg, 100% ($n=4$–9). The LD_{50} for i.p. administration of L-lysine is somewhere around 2.5–3 g/kg. Rats usually died within 2–3 h following injection after developing lethargy, neurological, and neuromuscular symptoms (tremor, twitching, and convulsions). In the rats that survived the L-lysine injection, pancreatic damage was assessed by histology. No pancreatic damage was detected in rats injected with 1 g/kg L-lysine ($n=6$, results not shown). Two out of 6 rats injected with 1.5 g/kg developed acute necrotizing pancreatitis. Ten out of 12 rats showed signs of severe necrotizing pancreatitis in the 2 g/kg group; the 2 remaining rats had no signs of pancreatitis on histological examination. The latter rats were excluded from the data analysis. Rats that survived the i.p. injection of 3–3.5 g/kg L-lysine developed acute necrotizing pancreatitis.

The reason why some rats in the 1.5 and 2 g/kg L-lysine groups did not develop pancreatitis is unknown; part of this may be due to technical problems (*e.g.,* L-lysine was injected into the bowel of rats). However, in accordance with these results, Bohus *et al.* (3) also found that about 15% of Sprague-Dawley rats were weak responders to high doses of L-arginine. These weak responders showed no signs of acute pancreatitis and had markedly lower excretion of L-arginine in the urine compared to the normal responders, indicative of more efficient detoxification of the amino acid *via* higher urea cycle and transaminase activities.

Similarly to our current findings, we and others have also observed lethality of rats after i.p. injection of large doses of L-arginine (>5 g/kg) (10, 31) and L-ornithine (4–6 g/kg) (28). The relatively sudden death of these rats is independent of acute pancreatitis and is likely to result from some metabolic complications.

Time course studies after i.p. injection of rats with 2 g/kg L-lysine

Macroscopic observations. The pancreas appeared edematous from 18 to 48 h, its peak being at 24 h. Abdominal fluid collection/accumulation was seen from 0.5 to 24 h. In the early time points this is likely to be unabsorbed L-lysine solution, and later on caused by ascites. Adhesions of organs were seen from 18 h to 24 h. Occasionally, yellow-white foci indicative of chalky fat necrosis was detected in the mesentery of the bowels and retroperitoneum at 24–72 h. Dilated small and large bowels suggesting functional ileus were apparent at 48 h–1 week after L-lysine injection.

Histological examination of the pancreas. Light microscopy: hematoxylin and eosin staining of a control pancreatic section is shown in Fig. 1A. Two hours after the i.p. injection of L-lysine (Fig. 1B), scattered delicate foamy vacuolization of the acini was observed, which progressed in size and extent from 4 to 9 h (Fig. 1C). The extent of apoptosis (as determined by the TdT-mediated dUTP nick end-labeling [TUNEL] technique) was significantly increased at 6 h (0.44% ± 0.07%) *versus* 0 h (0.13% ± 0.01%) ($n=3$–4). At 12 h, foamy vacuolization disappeared, and interstitial edema, neutrophilic and monocytic adherence, and focal infiltration were observed. Acinar cell necrosis was evident; increasing number of widespread apoptotic bodies could also be detected (1.02% ± 0.19%). At 24 h, the degree of pancreatic edema was greatly increased (Fig. 1D). There was moderate diffuse infiltrate of monocytes and neutrophils. Widespread acinar cell necrosis was observed; the extent of apoptosis was 0.58% ± 0.05%. At 48 h, inflammatory (monocytic and neutrophilic) infiltration reached its maximum level (Fig. 1E). Some fibroblasts appeared in the interstitium; the lobular architecture of the pancreas was distorted. Necrotic and apoptotic processes were decreased; ductuloacinar structures, indicative of regeneration, appeared in the peripheral region of the pancreas. At 72 h after injection, diffuse severe infiltrate of fibroblasts, macrophages/monocytes, eosinophils, and neutrophils was evident (Fig. 1F). The extent of apoptosis was relatively high (1.59% ± 0.05%). There was a mild degree of collagen deposition within the lobules and around ductuloacinar structures. Ductuloacinar structures with mitotic figures were budding from the tubular lumina. At 1 week, diffuse moderate infiltrate of fibroblasts and macrophages along with relatively smaller number of eosinophils and neutrophils were observed (Fig. 1G). The extent of apoptosis was 1.39% ± 0.18%. There was a mild deposition of collagen within the lobules and around ductuloacinar structures. Some of the destructed lobules were replaced by adipose tissue. Budding ductuloacinar structures started to form ductules and acini. Dilation of the small ducts and ductules was observed, which—in some cases—contained eosinophilic material. One month after L-lysine injection, the pancreas appeared almost normal, except that part of the parenchyma was replaced by fat (Fig. 1H). The acini showed numerous mitotic figures and regenerative atypia.

Table 1 shows a summary of pancreatic histopathological changes in response to injection of L-lysine. Overall, there were no major pathologic alterations of the pancreatic duct cells and islets of Langerhans. Notably, acini surrounding Langerhans islets were relatively preserved from injury. Some animals showed Langerhans islet hyperplasia at 1 month.

Diaphorase enzyme histochemistry: In pancreatic sections from control rats, diaphorase enzyme histochemistry revealed dark blue rod-shaped structures (0.94 ± 0.03 μm in length, $n=43$), arranged at the basal compartment of the acinar cells decisively at the perinuclear region, which are likely to be mitochondria (Fig. 2A). At 2 h after L-lysine

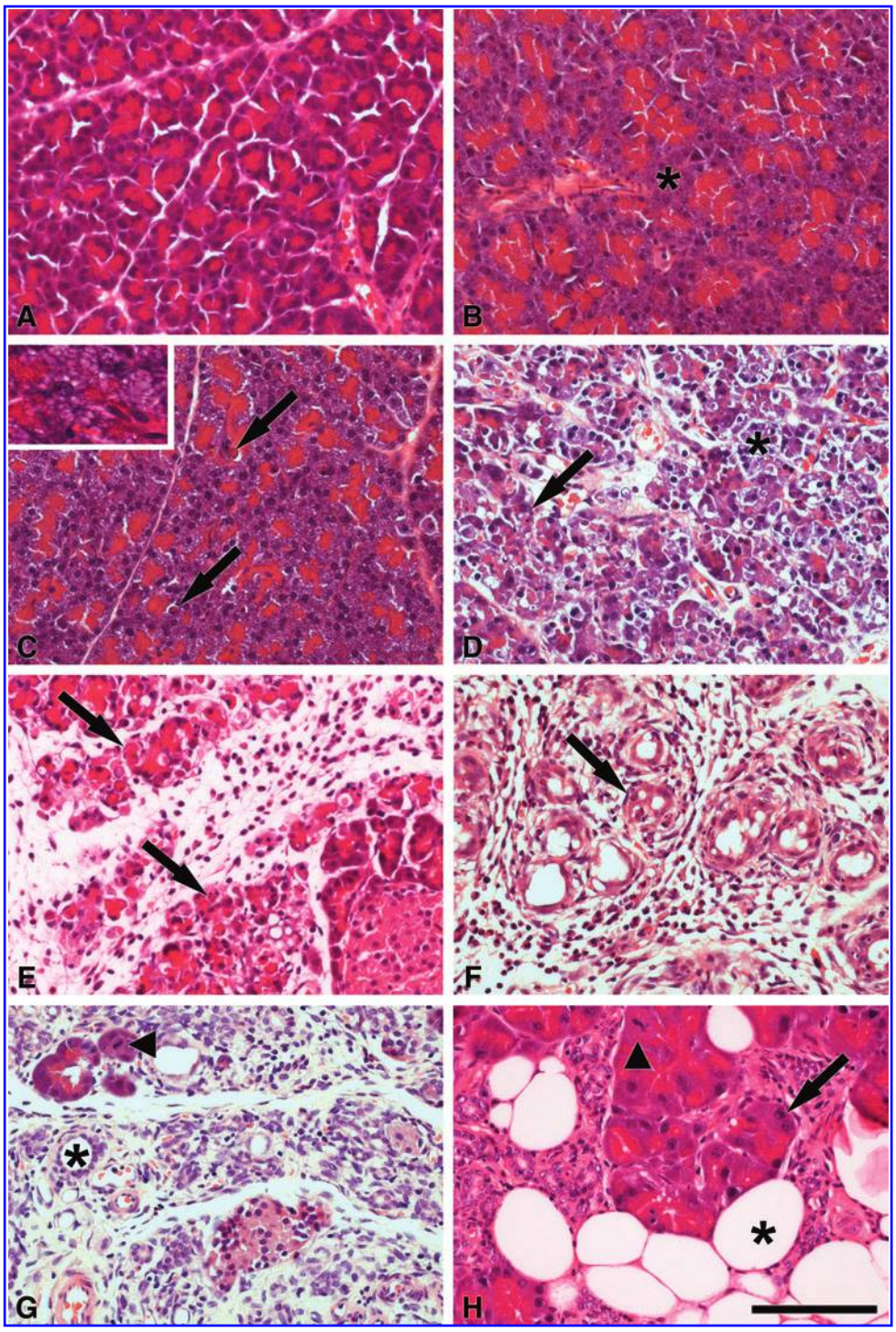

FIG. 1. Histopathological changes of the pancreas in response to intraperitoneal administration of 2 g/kg L-lysine. (A) 0 h (control pancreatic section). **(B)** 2 h: Foamy degeneration (*asterisk*) of acinar cells was observed. **(C)** 6 h: Massive foamy degeneration (*inset*) of acinar cells, *arrows* indicate apoptotic bodies. **(D)** 24 h: Widespread necrosis of acinar cells (*asterisk*) and lots of apoptotic bodies (*arrow*). **(E)** 48 h: Necrobiotic processes of acini (*arrows*); inflammatory cell infiltration is prominent in the edematous interstitium. **(F)** 72 h: Ductuloacinar structures (*arrow*) replaced damaged acini, fibroblasts, macophages and neutrophils in the interstitium. **(G)** 1 week: Some acini have regenerated (*arrow*) with mitotic figures (*arrowhead*) between the ductuloacinar structures (*asterisk*). **(H)** 1 month: Acini (*arrow*) show mitotic figures (*arrowhead*) and regenerative atypia; fatty tissue (*asterisk*). Scale bar = 100 μm. (To see this illustration in color the reader is referred to the web version of this article at www.liebertonline.com/ars).

injection, besides the dark blue rod-shaped structures, light blue, larger, rod-shaped structures or spheroid vesicles (1.45 ± 0.06 μm in length, $n = 42$) were observed (Fig. 2B). The latter are indicative of hydropic degeneration. Note that the nucleus of acinar cells was also slightly larger. At 24 h after L-lysine injection, enzyme histochemistry revealed shrunken nuclei and nearly total disappearance of diaphorase staining (Fig. 2C).

Electron microscopy: Figure 3A and B shows representative pictures of pancreatic acinar cells from control animals. The length of control mitochondria was 0.740 ± 0.034 μm ($n = 37$). At 6 h after L-lysine treatment, pancreatic acinar mitochondria showed progressive hydropic degeneration (Fig. 3C, D). Their length was increased by almost 3-fold to 2.098 ± 0.068 μm ($n = 62$). An inchoate condensation of chromatin beneath the nuclear membrane could also be observed but the rough endoplasmic reticulum and zymogen granules were unaltered.

At 24 h, there was extensive damage of the acini (Fig. 3E, F). First, shrinkage of the cytoplasm and disappearance of the nucleoli along with coarse condensation of the chromatin beneath the nuclear membrane was evident. Second, large

Table 1. Evaluation of Pancreatic Injury by Histological Examination 2–168 h and 1 Month After Intraperitoneal Injection of Rats with 2 g/kg L-Lysine

	2 h	*4 h*	*6 h*	*9 h*	*12 h*	*18 h*	*24 h*	*48 h*	*72 h*	*168 h*	*1 month*	*kappa*
Hyperaemia	0	1	1	1	1	1	1	1	1	1	1	0.769
Interstitial edema	1	1	1	2	1	2	3	3	1	1	0	0.702
Leukocyte adherence	0	1	1	2	2	3	3	3	3	3	0	0.735
Leukocyte infiltration	0	0	0	1	2	2	4	4	4	4	0	0.684
Vacuolization/foamy degeneration	3	4	4	4	2	0	0	0	0	0	0	0.814
Necrosis	0	0	0	0	1	2	4	2	1	0	0	0.764
Apoptosis	0	0	1	2	2	1	2	1	2	1	0	0.713
Regeneration	0	0	0	0	0	0	0	0	1	1	0	0.659

The histopathological scores of five to six rats were the result of agreement between the two pathologists. Values for control animals (injected intraperitoneally with physiological saline instead of L-lysine) were 0. The weighted-kappa values indicate substantial agreement between the two observers.

autophagic vacuoles containing zymogen granules, myelin figures, and lipid droplets of medium density and nearly complete disappearance of mitochondria were also seen. Rough endoplasmic reticulum showed dilation and separation of ribosomes. Increased numbers of neutrophils and monocytes were observed in the interstitial space.

At 1 week, low-power electron micrographs revealed increased number of capillaries, several ductuloacinar structures, mononuclear cells, and collagen in the interstitial space. The ductuloacinar structures were tortuous, and frequently differentiated into acinar cells with a few zymogen granules, and ductuli (Fig. 3G, H). Occasionally, mitosis of epithelial cells was encountered. Some cells were enlarged and contained huge number of small electron-dense granules, indicating ductoendocrine proliferation.

The mitochondria of pancreatic ductal and islet cells were not affected (results not shown).

Light microscopic examination of the kidney, lung, and liver. At 9–48 h after the injection of 2 g/kg L-lysine, progressive attenuation or loss of proximal tubule brush borders, vacuolization, and swelling of these cells were seen. Some eosinophilic and pigmented granular casts in the tubular lumina were observed particularly in distal tubules of the kidneys. Further, accumulation of leukocytes within and around the dilated peritubular capillaries also was found, consistent with acute tubular necrosis. At the same time in the lungs, the alveolar septa showed varying amounts of interstitial edema that was usually accompanied by infiltration of polymorphonuclear leukocytes and scant numbers of lymphocytes and plasma cells. Edema in the alveolar space and alveolar thickening with hyperplasia of alveolar type II cells were seen indicative of early exudative phase of diffuse alveolar damage. No conspicuous alterations were observed in the liver.

Assessment of $\Delta\Psi m$ and oxygen consumption of isolated pancreatic and liver mitochondria. We used 2 approaches to examine the effect of L-lysine on pancreatic and liver mitochondria. First, we added exogenous L-lysine to the suspension of the mitochondria isolated from control animals, and measured its effect on the mitochondrial membrane potential and O_2 consumption. Second, the same parameters were measured in mitochondria isolated from animals which received an i.p. injection of L-lysine (2 g/kg).

Rat pancreatic mitochondria (RPM) and rat liver mitochondria (RLM) isolated from control animals ($n=3$) displayed stable mitochondrial membrane potential ($\Delta\Psi m$) and oxygen consumption (Fig. 4). Addition of exogenous adenosine diphosphate (ADP) stimulated oxidative phosphorylation in RPM (Fig. 4A) and RLM (results not shown) manifested by reduced $\Delta\Psi m$ and increased respiration rate. When ADP is consumed, $\Delta\Psi m$ and the respiration rate return to the basal levels. The mitochondrial uncoupler dinitrophenol (DNP) was added to completely dissipate $\Delta\Psi m$. L-lysine at 30–60 m*M* concentrations did

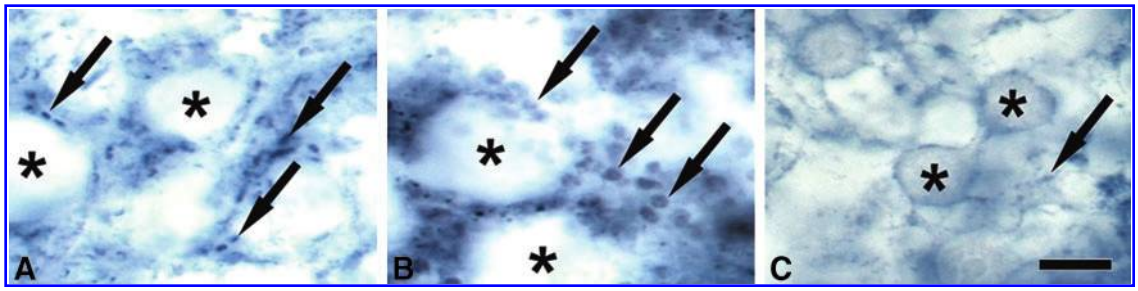

FIG. 2. $NADH_2$ diaphorase staining of pancreatic tissue shows swollen mitochondria in rats treated with L-lysine. To stain mitochondria, diaphorase enzyme histochemistry was performed on pancreatic tissue obtained from control **(A)** and L-lysine-treated (2 g/kg i.p.) **(B, C)** rats. **(A)** In control pancreatic sections, dark blue rod shaped mitochondria were arranged at the basal compartment of the acinar cells decisively at the perinuclear region. **(B)** 2 h after L-lysine injection, beside rod-shaped mitochondria, light blue, spheroid vesicles could be observed. The latter are indicative of hydropic degeneration and damaged mitochondrial function. **(C)** 24 h after L-lysine injection, we observed shrunken nuclei and nearly total disappearance of mitochondria. The *arrows* and *asterisks* indicate mitochondria and nuclei, respectively. Scale bar = 6 μm. (To see this illustration in color the reader is referred to the web version of this article at www.liebertonline.com/ars).

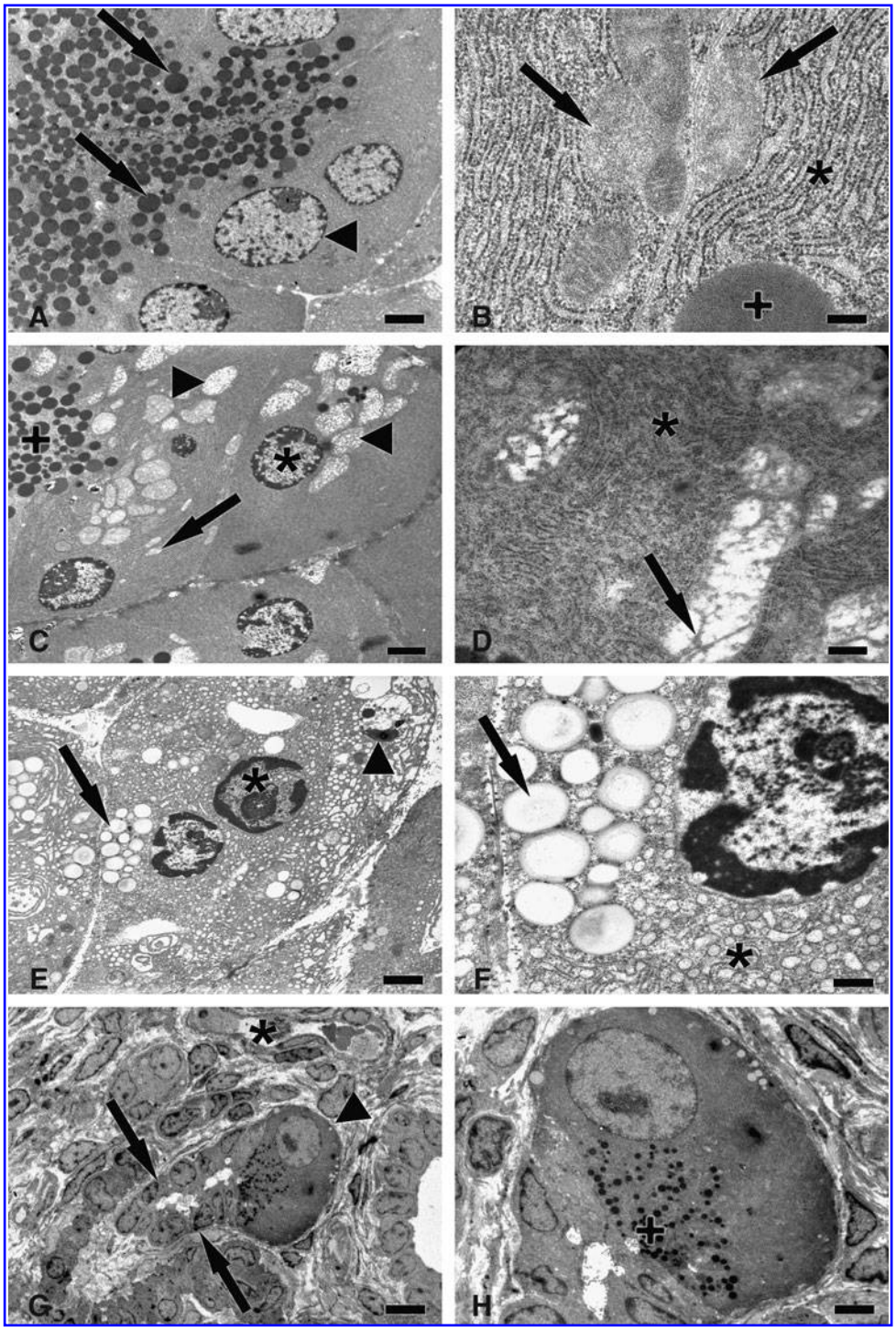

FIG. 3. Electron micrographs of the rat pancreas 0 h (A, B), 6 h (C, D), 24 h (E, F), and 1 week (G, H) after intraperitoneal administration of 2 g/kg L-lysine ($n = 3$). (A) Cell nucleus (*arrowhead*) and zymogen granules (*arrow*) (scale bar = 2 μm). **(B)** Mitochondria (*arrows*), rough endoplasmic reticulum (*asterisk*), and zymogen granule (*cross*) (scale bar = 0.2 μm). **(C)** Mitochondria displaying progressive degeneration (*arrow*); the length of some (*arrowheads*) almost reach the diameter of the nucleus (*asterisk*); unaltered zymogen granules (*cross*) (scale bar = 2.5 μm). **(D)** Degenerated mitochondrion with recognizable cristae (*arrow*); disorganized rough endoplasmic reticulum (*asterisk*) (scale bar = 0.4 μm). **(E)** Nucleus with peripheral compacted chromatin (*asterisk*); myelin figures (*arrowhead*) and lipid droplets of medium density (*arrow*) (scale bar = 2.5 μm). **(F)** Dilated rough endoplasmic reticulum (*asterisk*); lipid droplets of medium density (*arrow*) (scale bar = 0.6 μm). **(G)** Ductuloacinar structure (*arrows*) differentiated into acinar cell (*arrowhead*); capillaries (*asterisk*) (scale bar = 7 μm). **(H)** Differentiated acinar cell with newly formed (*cross*) zymogen granules (scale bar = 3 μm).

not affect the respiration rate of RPM (Fig. 4B) and RLM (Fig. 4C), and only slightly reduced $\Delta\Psi$m. However, exogenous L-lysine significantly inhibited the rate of $\Delta\Psi$m recovery after consumption of ADP in RPM (Fig. 4B). Similar inhibition of $\Delta\Psi$m recovery after addition of ADP was observed in RPM 1 h (Fig. 4D) and 4 h (Fig. 4E) after L-lysine injection; the effect was more pronounced at 4 h after injection. In accord with these data, we found that the rate of oxygen consumption remained elevated in mitochondria from rats injected with L-lysine even after the synthesis of adenosine triphosphate (ATP) was finished. The data suggest that L-lysine impairs coupling of electron transport chain or causes disbalance between ATP hydrolysis and synthesis. Importantly, L-lysine had no effect on $\Delta\Psi$m and oxygen consumption recovery in RLM (Fig. 4C, F), indicating selective damage of pancreatic mitochondria.

Pancreatic weight/body weight ratio, activities of serum amylase, lipase, and pancreatic amylase, trypsin, and myeloperoxidase. We observed a biphasic increase followed by a decrease in pancreatic weight/body weight ratio (p.w./b.w.) in response to i.p. injection of 2 g/kg L-lysine (Fig. 5A). p.w./b.w. initially (2–9 h) increased and then

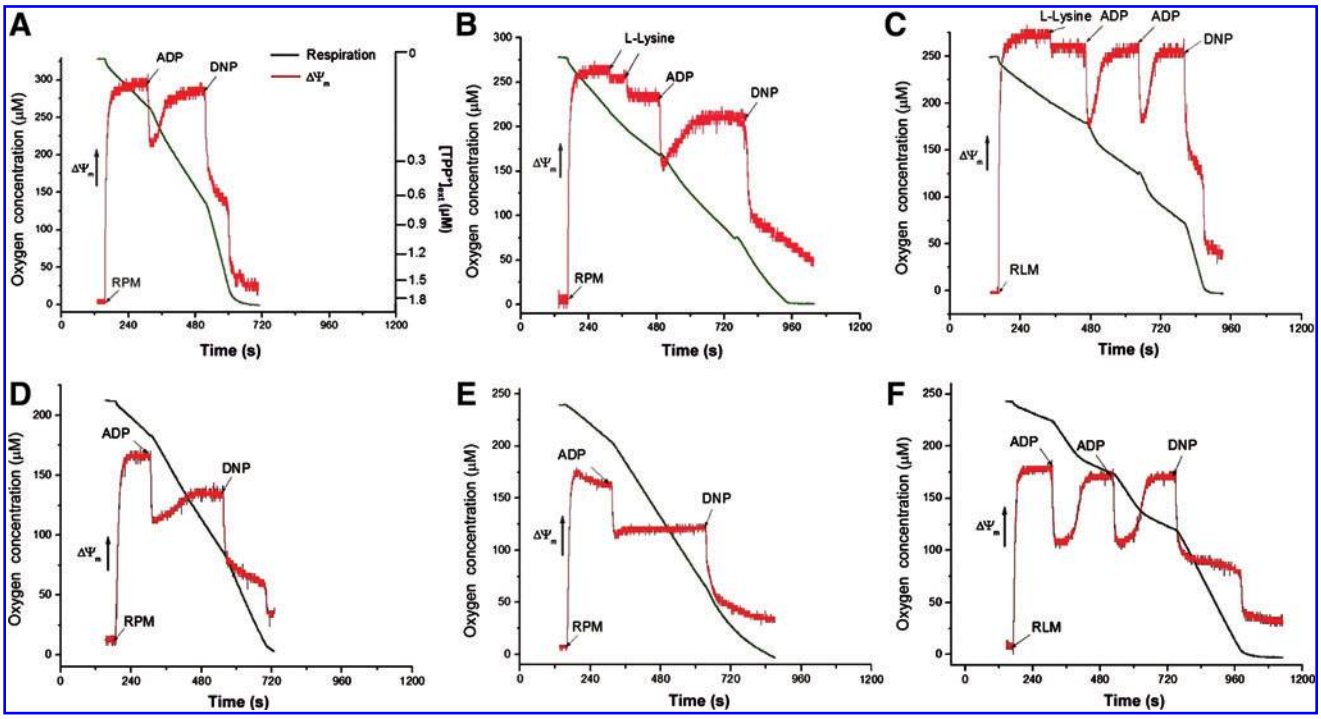

FIG. 4. L-lysine inhibits the recovery of mitochondrial membrane potential after addition of adenosine diphosphate (ADP). Rat pancreatic mitochondria (RPM) and liver mitochondria (RLM) were isolated **(A–C)** 0, **(D)** 1, or **(E, F)** 4 h after the i.p. injection of 2 g/kg L-lysine as described in Odinokova *et al.* (23). Mitochondrial membrane potential (ΔΨm, *red line*) and oxygen consumption (*green line*) were measured in RPM or RLM suspension with tetraphenyl phosphonium ion (TPP^+) and Clark electrodes, respectively. Mitochondria (RPM or RLM), ADP (20 μM), L-lysine (30–60 mM), and the mitochondrial uncoupler dinitrophenol (DNP, 5 μM) were added as indicated. Mitochondria displayed stable ΔΨm and oxygen consumption. The addition of ADP to **(A)** RPM and RLM (results not shown) reduced ΔΨm and increased oxygen consumption which eventually recovered to control levels. **(B)** 2 × 30 mM or **(C)** 1 × 60 mM L-lysine did not affect the respiration of **(B)** RPM and **(C)** RLM, but slightly reduced ΔΨm. Importantly, L-lysine significantly inhibited the rate of ΔΨm recovery in **(B)** RPM, but not in **(C)** RLM. In RPM isolated from L-lysine-treated (2 g/kg i.p.) animals **(D)** 1 h or **(E)** 4 h after injection, the rate of ΔΨm recovery in response to 20 μM ADP was significantly decreased after addition of ADP. **(F)** ΔΨm recovery was not affected in RLM isolated 4 h after the injection of L-lysine. Similar results were found in RLM isolated 1 h after the injection of L-lysine (data not shown). Traces are representative of 3 independent experiments. (To see this illustration in color the reader is referred to the web version of this article at www.liebertonline.com/ars).

returned to control levels (12 h), which correlated well with the appearance and then disappearance of foamy degeneration (mitochondrial swelling) of acinar cells. p.w./b.w. was then (18–48 h) significantly increased by pancreatic edema, but significantly decreased below control levels thereafter (due to almost complete destruction of pancreatic acini).

The serum amylase and lipase activities were significantly increased at 12–24 h (Fig. 5B, C). Pancreatic amylase activity was significantly decreased from 24 h to 1 week after L-lysine injection (Fig. 5D). Pancreatic trypsin activity was significantly decreased at 0.5–2 h and significantly increased 12–24 h after i.p. injection of L-lysine (Fig. 5E). Pancreatic myeloperoxidase (MPO) activity was significantly increased from 18 to 72 h and returned to basal values 168 h after the injection of L-lysine.

Induction of pancreatic heat-shock protein 72 synthesis. Inducible heat-shock proteins such as heat-shock protein 72 (HSP72) are sensitive markers of pancreatic injury (26). HSP72 could not be detected in the physiological saline (PS)-treated control group (Fig. 6A). However, by 4 h after the injection of 2 g/kg L-lysine, the level of HSP72 was significantly increased, peaked at 12–18 h and remained elevated until 168 h.

Pancreatic levels of IκB-α and interleukin-1β. A key factor in regulating NF-κB activation is the degradation of IκB-α (27). Pancreatic IκB-α levels were significantly decreased from 18 to 72 h in response to L-lysine injection (Fig. 6B). Corresponding to IκB degradation and the consequent activation of NF-κB, pancreatic interleukin (IL)-1β synthesis significantly increased from 18 to 72 h (Fig. 6C).

Pancreatic nonprotein sulfhydryl group content, and the activities of glutathione peroxidase and superoxide dismutase. The GSH-Px activity and nonprotein sulfhydryl group (NSG) content were significantly increased at 24–48 and 24–72 h (respectively) in the L-lysine-treated group compared with the control group (Fig. 7A, B). Mn-superoxide dismutase (SOD) activity was significantly increased at 18 h and significantly decreased at 168 h *versus* the control (Fig. 7C). In contrast, the activity Cu/Zn-SOD was significantly increased 18–24 h (Fig. 7D).

Pancreatic spermidine/spermine N^1-acetyltransferase activity and polyamine levels. Interestingly, there was a biphasic activation of pancreatic spermidine/spermine N^1-acetyltransferase (SSAT) activity in response to L-lysine

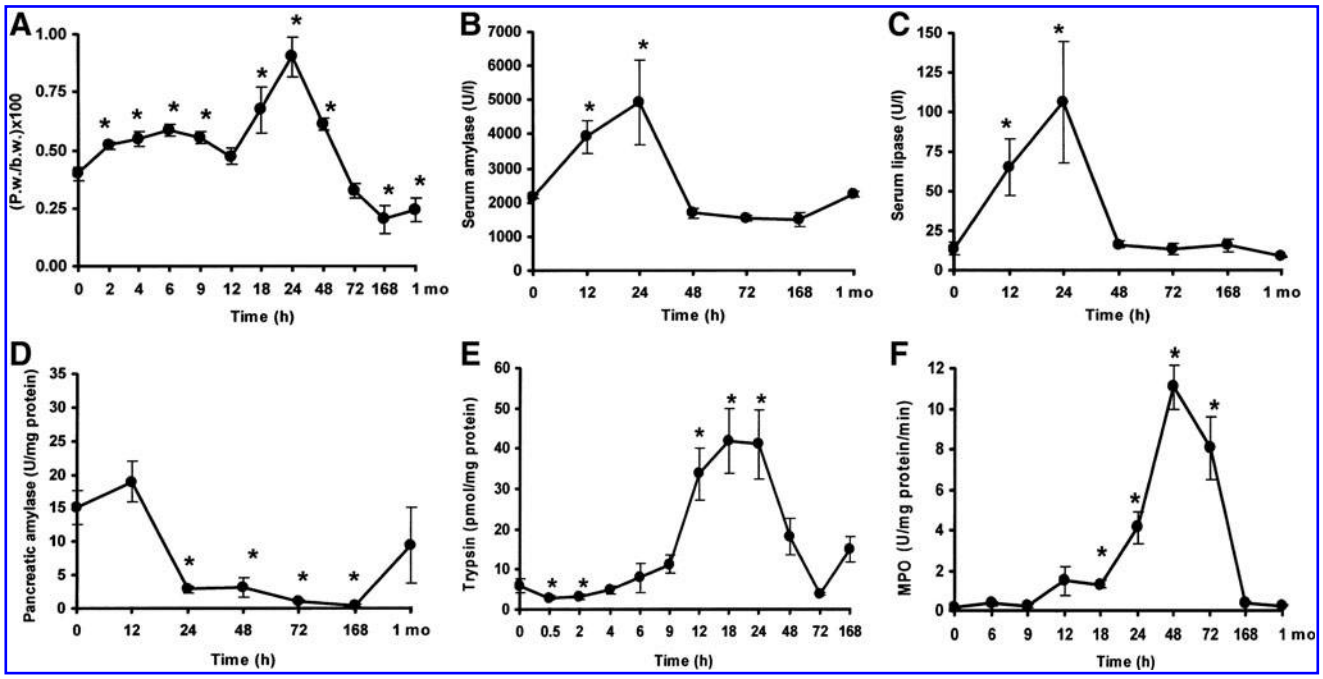

FIG. 5. Time course of pancreatic weight/body weight ratio (p.w./b.w.), activities of serum amylase, lipase and pancreatic amylase, trypsin, and myeloperoxidase (MPO) after i.p. administration of 2 g/kg L-lysine. (A) p.w./b.w. and activities of serum **(B)** amylase, **(C)** lipase and pancreatic **(D)** amylase, **(E)** trypsin, and **(F)** MPO. Data are shown as means ± SEM, $n = 4$–12. *Significant difference ($p < 0.05$) *versus* the control group (0 h).

administration (Fig. 8A). The first peak was observed at 12 h, and the second at 48–72 h. Correspondingly, spermidine levels were significantly decreased from 24 to 168 h (Fig. 8B). Spermine levels were unaltered by L-lysine treatment; putrescine could not be detected (data not shown).

Serum aspartate amino transferase activity and concentrations of urea, creatinine, glucose, calcium, and triglyceride. Serum aspartate amino transferase (ASAT) activity was significantly increased by about 2–3-fold at 12–48 h after L-lysine injection (Fig. 9A). Serum urea and creatinine concentrations were significantly increased at 24 h (Fig. 9B, C). Serum concentrations of glucose were significantly decreased from 24 to 48 h, and returned to normal by 72 h (Fig. 9D). The decreased serum glucose concentration is likely to be due to anorexia of rats. Calcium and triglyceride concentrations were not influenced by the administration of L-lysine (results not shown).

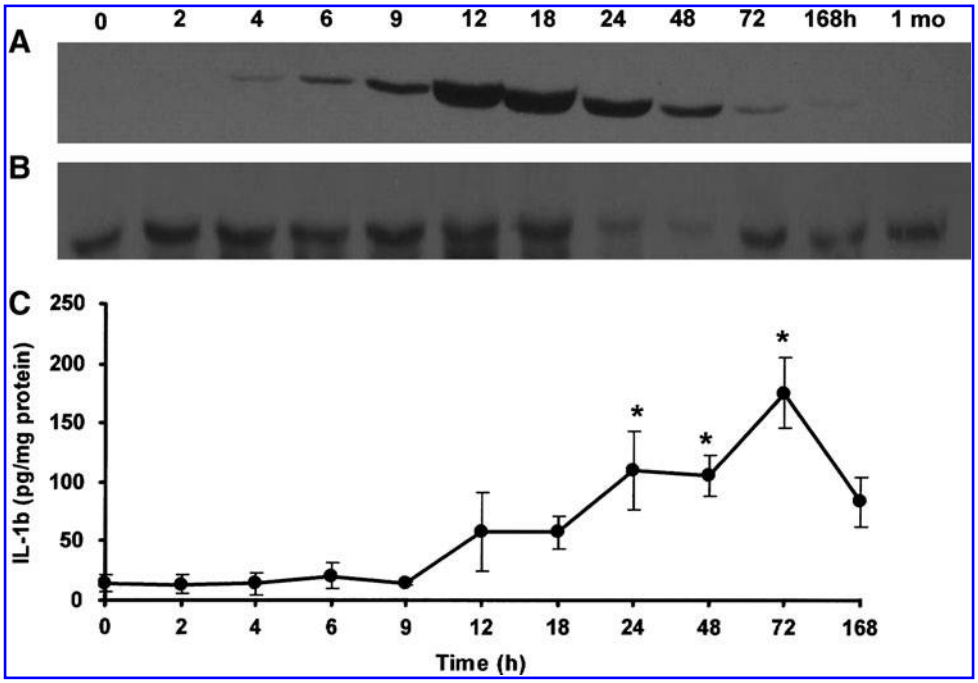

FIG. 6. Effects of L-lysine administration (2 g/kg i.p.) on pancreatic heat-shock protein 72 (HSP72), IκB-α, and interleukin (IL)-1β expression as a function of time. (A, B) Representative Western immunoblot analysis of protein lysates (40 μg/lane) from the pancreata of rats 0–168 h and 1 month after injection, showing the levels of **(A)** HSP72 and **(B)** IκB-α as a function of time. **(C)** The graph shows the expression of the proinflammatory cytokine, IL-1β as determined from the cytosolic fractions of pancreatic homogenates by ELISA. Means ± SEM for 4–6 animals are shown. *Significant difference ($p < 0.05$) *versus* the control group (0 h).

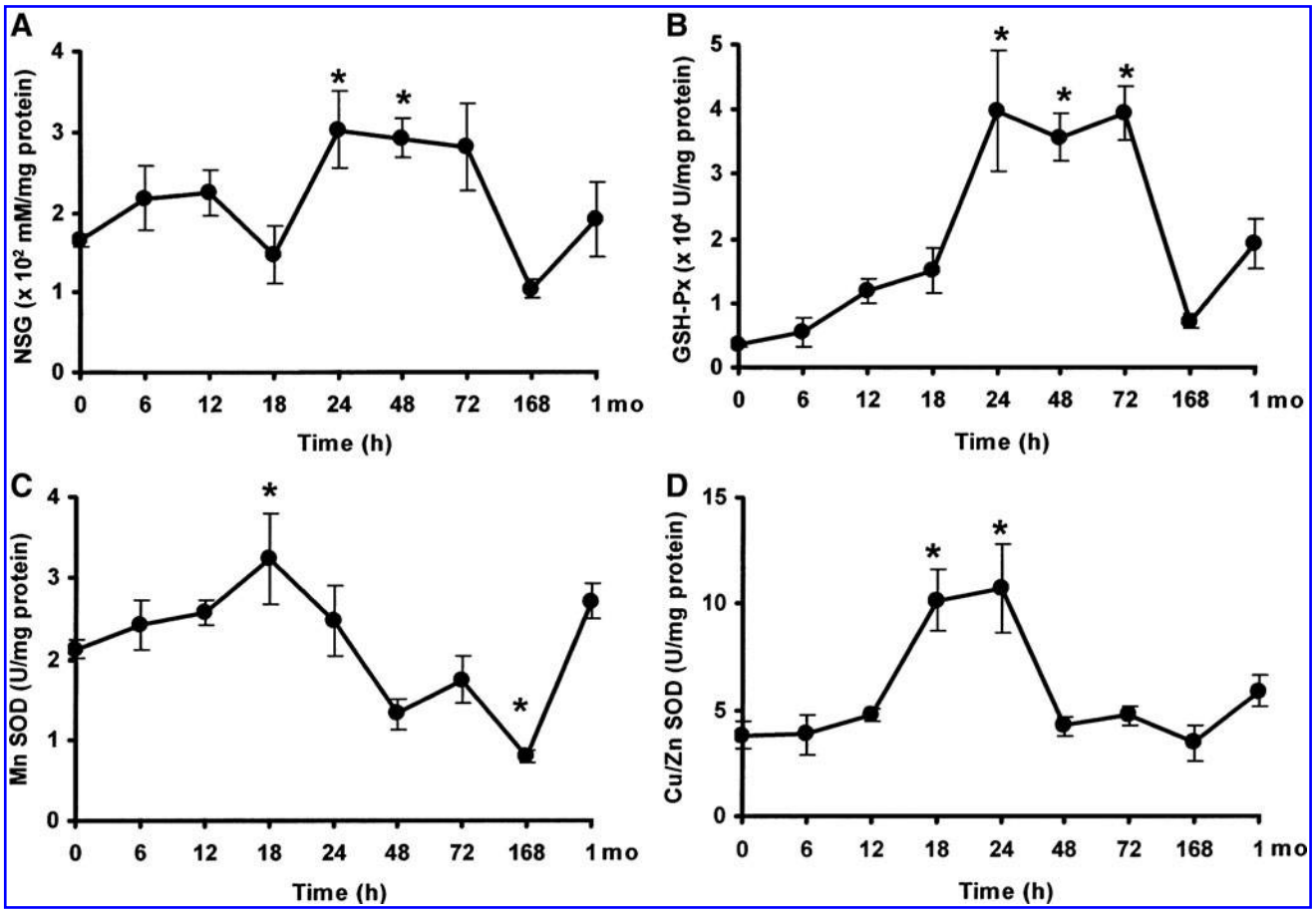

FIG. 7. L-lysine injection (2 g/kg intraperitoneally) induces pancreatic oxidative stress. Changes in pancreatic **(A)** non-protein sulfhydryl group (NSG) content, **(B)** glutathione-peroxidase (GSH-Px), **(C)** Mn, and **(D)** Cu/Zn superoxide dismutase (SOD) are shown. Means ± SEM for 5–6 animals are shown. *Significant difference ($p < 0.05$) *versus* the control group (0 h).

Discussion

Large doses of basic amino acids such as L-arginine and L-ornithine have been shown to induce acute experimental pancreatitis (10, 28). The basic L-lysine seemed to be an exception. In fact, the i.p. injection of L-lysine was reported to cause pancreatic necrosis without inflammatory cell infiltration, which is a peculiar finding (14, 15).

In this study we showed that L-lysine also causes acute necrotizing pancreatitis in rats manifested by serum hyperamylasemia, trypsinogen activation, inflammatory infiltration, and acinar cell death through necrosis and apoptosis. Thus, our

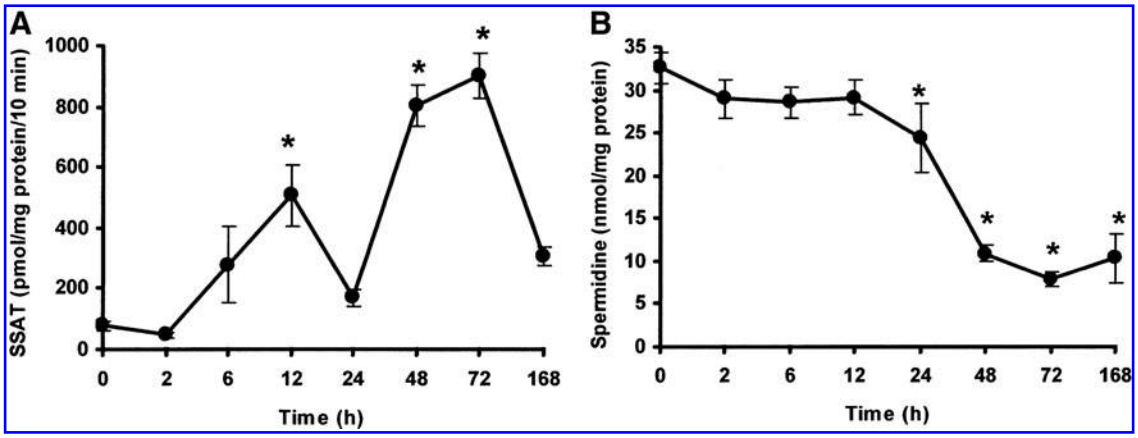

FIG. 8. Intraperitoneal injection of 2 g/kg L-lysine induces pancreatic polyamine catabolism. The figure shows **(A)** spermidine/spermine N^1-acetyltransferase (SSAT) activity and **(B)** spermidine levels. Spermine levels were unaltered by L-lysine treatment, putrescine could not be detected (data not shown). Data are presented as means ± SEM, $n = 5–6$. *Significant difference ($p < 0.05$) *versus* the control group (0 h).

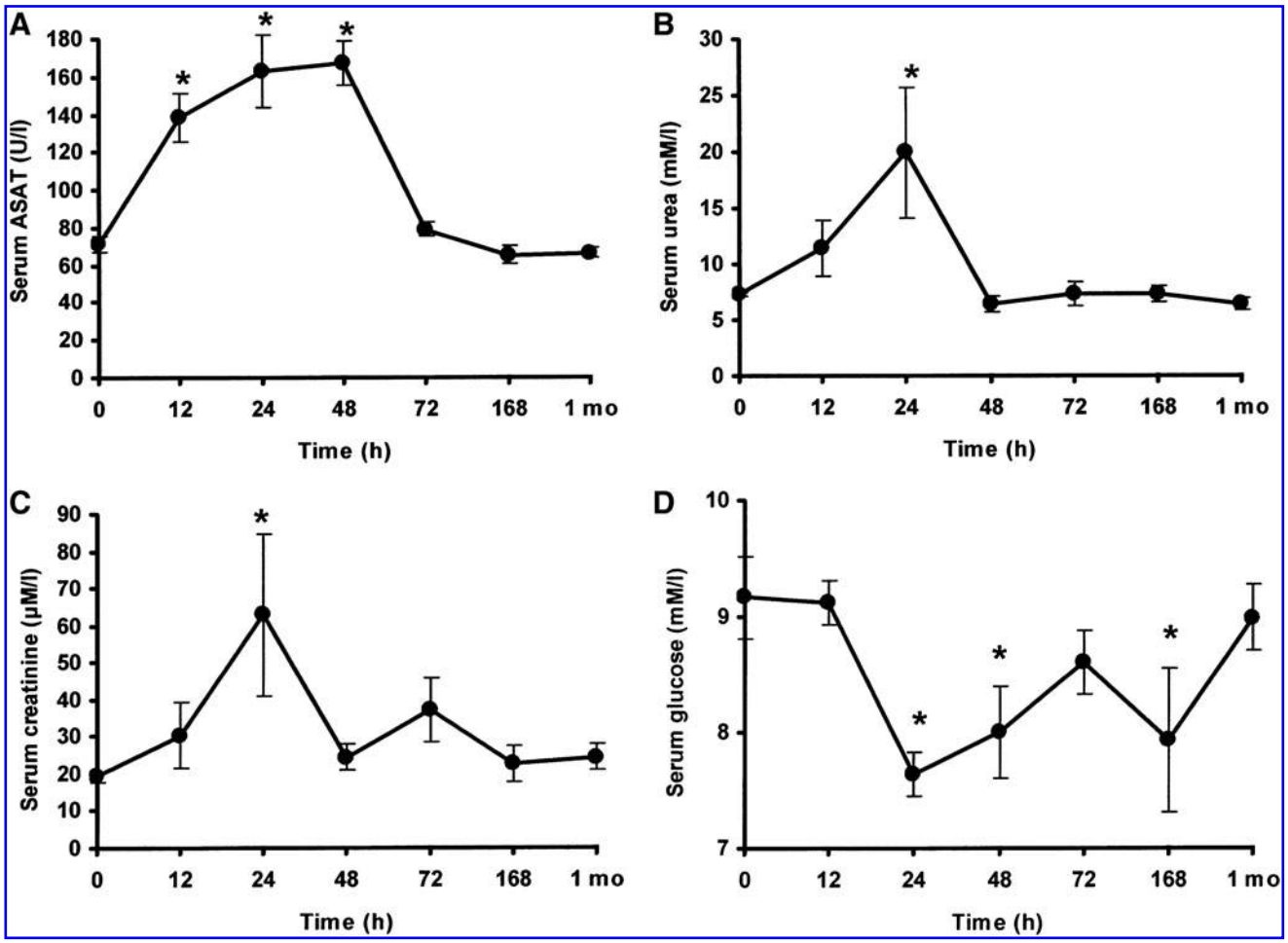

FIG. 9. Time course changes of serum aspartate amino transferase (ASAT) activity and concentrations of urea, creatinine, and glucose after intraperitoneal administration of 2 g/kg L-lysine. Serum **(A)** ASAT activity and concentrations of **(B)** urea, **(C)** creatinine, and **(D)** glucose. Data are shown as means ± SEM, $n = 5–6$. *Significant difference ($p < 0.05$) *versus* the control group (0 h).

previous and current data demonstrate that basic amino acids L-ornithine, L-arginine, and L-lysine induce acute pancreatitis-like changes in the exocrine pancreas (26, 28). The effect was specific for the pancreas, as these amino acids produced only mild or no toxic effects on the liver, or other organs. The latter are most likely due to secondary effects of acute pancreatitis, as they occur well after the initiation of the disease. The mechanisms of basic amino acid-induced toxicity on the exocrine pancreas are yet to be determined. However, our data suggest mitochondrial dysfunction as a possible trigger of L-lysine-induced pancreatitis. Electron microscopy showed that massive swelling of mitochondria is already evident at early time points. Similar finding was reported previously (14, 15). The experiments on the pancreatic mitochondria isolated from control and L-lysine-treated rats show that L-lysine impairs the function of ATP synthase, either by impairing coupling of electron transport chain or by causing disbalance between ATP hydrolysis and synthesis. Indeed, we found that mitochondria fail to restore normal potential and respiration after ADP addition. Further, L-lysine selectively damages pancreatic mitochondria; it had no effect on the liver mitochondria. This may be because properties of pancreatic and liver mitochondria are different (23). Odinokova *et al.* found that pancreatic mitochondria are more sensitive to Ca^{2+} than liver mitochondria and maintain their functional state only if isolated in the presence of EGTA (23). Further, it was demonstrated that the permeability transition pore (mPTP) in pancreatic mitochondria has unusual properties, different from the liver mPTP. A key characteristic of liver mPTP opening is mitochondria swelling, leading to outer mitochondrial membrane rupture. In contrast, mPTP opening in isolated pancreatic mitochondria was not associated with swelling. Further, in pancreatic mitochondria Ca^{2+}-induced depolarization caused a dramatic decrease in production of reactive oxygen species, in contrast with reactive oxygen species burst induced by mPTP opening in mitochondria from liver. Mitochondrial depolarization and subsequent detrimental effects to acinar cells in response to a variety of pancreatic toxins used in most other pancreatitis models are thought to be from large rises in cytosolic calcium (25). Therefore, the effect of administering high concentrations of basic amino acids on acinar cytosolic calcium concentration needs to be tested.

Importantly, mitochondrial injury occurs early and precedes the activation of trypsinogen and NF-κB, which are commonly thought as initiating events of acute pancreatitis. In accordance with the latter findings, trypsinogen and NF-κB activation also occurred at a later phase in L-arginine and

L-ornithine-induced acute pancreatitis (26, 28). Paradoxically, pancreatic trypsin activity was initially decreased soon (0.5–2 h) after the injection of 2 g/kg L-lysine and increased only from 12 h.

Mitochondrial dysfunction is a critical mediator of acinar cell death in pancreatitis (22). In accord with the mitochondrial damage, we found that L-lysine greatly increased acinar cells necrosis and apoptosis. Similarly, both necrosis and apoptosis were upregulated in models of pancreatitis induced by L-arginine or L-ornithine (16, 28). Thus, despite mitochondrial damage, acinar cells of L-lysine-treated rats maintain sufficient level of ATP to stimulate apoptosis (which is energy dependent).

Induction of severe acute pancreatitis was most effective with i.p. injection of 2 g/kg L-lysine. Pathologic parameters of acute pancreatitis induced by L-lysine were typical of acute pancreatitis. L-lysine selectively damaged pancreatic acinar cells without any major pathological alterations of the duct cells and islets of Langerhans. There was no evidence of hyperglycemia/diabetes mellitus after acute pancreatitis. As we discussed above, the earliest damaging effect was on mitochondria, at 1 h after L-lysine injection. Induction of pancreatic HSP72 synthesis, a sensitive indicator of pancreatic injury, was already detected at 4 h. Trypsinogen activation was maximal at 12–24 h; at the same time we detected maximal increase in serum amylase activity associated with a parallel decrease in pancreatic amylase activity. Acinar cell necrosis was evident from 12 h. Pancreatic NF-κB activation, proinflammatory cytokine induction, and increased MPO activity, indicators of the inflammatory response, as well as oxidative stress and spermidine depletion (possibly mediated through activation of SSAT) were prominent after 18 h.

Our findings on the toxic effects of L-lysine on the pancreas are partly supported by Kitajima and Kishino (15), who 25 years ago reported that L-lysine caused pancreatic acinar cell necrosis and increased serum amylase and lipase activities. Notably, Kitajima and Kishino injected male Wistar rats with 4 g/kg L-lysine-HCl i.p.; however, rats were fasted for 15 h before the injection, and the concentration of the L-lysine-HCl (rather than L-lysine) solution was more dilute (20% w/v) than ours (30% w/v).

In conclusion, we characterized a novel model of severe necrotizing acute pancreatitis induced by L-lysine. The results of this study, in combination with our previous data, indicate that basic amino acids, L-lysine, L-arginine, and L-ornithine, all injure the exocrine pancreas, resulting in pancreatitis. Our data demonstrate that L-lysine impairs ATP synthase activity of pancreatic mitochondria. This occurs early in the development of the disease and is followed by trypsinogen and NF-κB activation inflammatory infiltration, and acinar cell death through apoptosis and necrosis. Importantly, L-lysine selectively damages pancreatic mitochondria; it had no effect on liver mitochondria. The data strongly suggest that mitochondrial damage is a cause of pancreatitis induced by L-lysine.

Materials and Methods

Materials

Laboratory chemicals were from Sigma-Aldrich Corporation (Munich, Germany) unless stated otherwise.

Experimental protocol

Animals. Male Wistar rats weighing 220–290 g were used. The animals were kept at a constant room temperature of 24°C with a 12-h light–dark cycle, and were allowed free access to water and standard laboratory chow (Biofarm, Zagyvaszántó, Hungary). The experiments performed in this study were approved by the Animal Care Committee of the University.

Dose response (n=4–12) and time course changes of L-lysine injection (n=5–10). To choose the most effective L-lysine dose for the time-course study, rats were injected i.p. with 1–5 g/kg body weight (b.w.) of L-lysine (cat no. 62840, dissolved in PS at a concentration of 300 mg/ml, pH 7.4) and were killed after 24 h. For the time-course study, rats were injected i.p. with 2 g/kg L-lysine. Rats were sacrificed after being anesthetized with 44 mg/kg pentobarbital by exsanguination through the abdominal aorta at 0.5–72 h, 1 week or 1 month after the L-lysine injection. The control animals received PS i.p. and were killed 24 h after the injection. The pancreas was quickly removed, cleaned from fat and lymph nodes, weighed, and frozen in liquid nitrogen and stored at -80°C until use. All blood samples were centrifuged at 2500 g for 20 min and the serum was stored at −25°C.

Histological examination

Light microscopy. A portion of the pancreas, lung, liver, and kidney was fixed in 6% neutral formaldehyde solution and subsequently embedded in paraffin. Sections were cut at 4 μm thickness and stained with hematoxylin and eosin. The slides were coded and read (20–30 high power fields/animal) by two independent observers who were blind to the experimental protocol. Pancreatic tissue injury was evaluated as follows: semiquantitative grading of interstitial edema (0–3), vascular congestion (0–1), leukocyte adhesion (0–3) and infiltration (0–4), vacuolization/foamy degeneration (0–4), apoptosis (0–3), and necrosis (0–4) of acinar cells was determined in each animal [described in more detail in Rakonczay *et al*. (28)]. Signs indicative of regeneration—mitotic figures, ductuloacinar structures, and basophilia of acinar cells—were recorded. The histopathological scores reported in the article were the result of agreement between the two pathologists (when the scores differed).

$NADH_2$ diaphorase assay. To stain mitochondria (7), diaphorase enzyme histochemistry was performed. Frozen pancreatic sections were cut at 10 μm thickness and warmed at room temperature for 30 min. The sections were then incubated in 0.1 *M* TRIS-HCl buffer (pH 7.0) containing 0.2 mg/ml nitro-blue tetrazolium, 0.125 mg/ml $NADH_2$, and 1.4 mg/ml KCN for 40 min at 37°C. The bluish precipitated formazan chelate was clearly visible under the light microscope. Staining was not observed in control sections using the latter solution without $NADH_2$.

Transmission electron microscopy. Approximately 1 mm^3 pieces of the pancreas were fixed in 3% phosphate-buffered glutaraldehyde at 6 h, 24 h, and 1 week after the i.p. administration of L-lysine. Tissue blocks were postfixed in 1% OsO_4, and then rinsed in distilled water, dehydrated in a

graded series of ethanol, and embedded in TAAB Transmit Resin (TAAB Laboratories, Reading, England). Ultrathin sections were double-stained with uranyl acetate and lead citrate and examined with a Philips electron microscope.

Assays

Activities of serum and pancreatic amylase, serum lipase, and ASAT and concentrations of glucose, calcium, triglyceride, urea, and creatinine. Laboratory parameters were determined as described previously (28).

Isolation of mitochondria, measurement of mitochondrial membrane potential, and respiration. RPM and RLM were isolated 0, 1, or 4 h after the i.p. injection of 2 g/kg L-lysine as described in Odinokova *et al.* (23). $\Delta\Psi$m and oxygen consumption were measured in RPM or RLM suspension with tetraphenyl phosphonium ion (TPP^+) and Clark electrodes, respectively. An increase in $\Delta\Psi$m causes TPP^+ uptake by mitochondria and a decrease of TPP^+ concentration in the media. Mitochondrial respiration was measured for indicated times in the presence of 10 m*M* succinate as a respiratory substrate. Quality of isolated mitochondria was assessed by measuring the ratio of oxygen uptake in the absence (respiratory control ratio) and in the presence of 20 μM ADP (normally, oxygen consumption rate is increased in response to addition of ADP due to ATP synthesis). Mitochondria use electrochemical gradient through $\Delta\Psi$m as energy to synthesize ATP. In other words, mitochondria consume $\Delta\Psi$m to synthesize ATP from ADP. After the process is finished $\Delta\Psi$m increases back to normal level.

Pancreatic weight/body weight ratio. This ratio was utilized to evaluate the degree of pancreatic edema.

Pancreatic trypsin activity. Trypsin activity in pancreatic tissue homogenates was measured as described previously (9). Briefly, the tissue was homogenized on ice in a buffer containing 5 m*M* MES, 1 m*M* $MgSO_4$, and 250 m*M* sucrose (pH 6.5). A 25-μL aliquot of the homogenate was incubated at 37°C for 300 s in assay buffer containing 50 m*M* Tris-HCl (pH 8.0), 150 m*M* NaCl, 1 m*M* $CaCl_2$, and 0.1 mg/ml bovine serum albumin and Boc-Gln-Ala-Arg-7-amino-4-methylcoumarin (a specific substrate for trypsin). Cleavage of this substrate by trypsin releases 7-amino-4-methylcoumarin, which emits fluorescence at 440 nm with excitation at 380 nm. Trypsin activity in each sample was determined using a standard curve for purified bovine trypsin.

Expression of pancreatic HSP72 and IκB-α. Western immunoblot analysis of pancreatic HSP72 and IκB-α expression was performed from the cytosolic fraction of the pancreas homogenate. Pancreatic cytosolic fractions were prepared as described previously (26). The protein concentration of the homogenate was determined by the method of Bradford (2). Forty micrograms of protein were loaded per lane. Samples were electrophoresed on an 8% sodium dodecylsulfate–polyacrylamide gel according to the method of Laemmli (19). The proteins on the gels were either stained with Coomassie Brilliant Blue (to demonstrate equal loading of proteins for Western blot analysis) or transferred to a nitrocellulose membrane for 1 h at 100 V. Equal transfer of proteins was verified by Ponceau S staining. Membranes were blocked in 5% nonfat dry milk (Biorad, Vienna, Austria) for 1 h, and incubated with rabbit anti-HSP72 [1:10,000 dilution, characterized previously by Kurucz *et al.* (18)] or anti-IκB-α (1:500 dilution; Santa Cruz Biotechnology, Santa Cruz, CA) antibody for an additional 1 h at room temperature. The immunoreactive protein was observed by enhanced chemiluminescence, using horseradish peroxidase-coupled anti-rabbit immunoglobulin at 1:10,000 dilution (Dako, Glostrup, Denmark).

Pancreatic IL-1β concentrations. The proinflammatory IL-1β concentrations were measured in the pancreatic cytosolic fractions with an ELISA kit (R&D Systems, Minneapolis, MN) according to the manufacturer's instructions.

Pancreatic NSG content, and the activities of glutathione peroxidase and superoxide dismutase. To determine parameters of oxidative stress, a part of the pancreas was homogenized, the homogenates were centrifuged at 3000 *g* for 10 min, and the supernatants were used for measurements as described previously (5). Briefly, NSG content was determined spectrophotometrically with Ellman's reagent (30). GSH-Px activity was determined according to the chemical method, using cumene hydroperoxide and glutathione as substrates of GSH-Px (4). SOD activity was determined on the basis of the inhibition of epinephrine-adrenochrome auto-oxidation (21). Mn-SOD activity was measured by the auto-oxidation method in the presence of 5 m*M* KCN (20). Cu/Zn-SOD activity was calculated by subtracting the activity of Mn-SOD from SOD activity.

Pancreatic polyamine levels and SSAT activity. The levels of natural polyamines (spermidine, spermine, and putrescine) were determined by high-performance liquid chromatography according to the method of Hyvönen *et al.* (12, 13). Pancreatic SSAT activity was assayed according to Bernacki *et al.* (1).

Pancreatic MPO activity. Pancreatic MPO activity, as a marker of tissue leukocyte infiltration, was assessed by the method of Kuebler *et al.* (17).

Detection of apoptosis in the pancreas. Cells showing characteristic changes of apoptosis were identified by light and electron microscopic techniques (see above). Apoptotic cells were quantitated by TUNEL technique using an In Situ Cell Death Detection Kit from Roche Diagnostics (Mannheim, Germany). Apoptotic cells were observed with 3,3′-diaminobenzidine (Dako, Glostrup, Denmark). The number of apoptotic cells was counted in 1 mm^2 of pancreatic tissue. Results are expressed as percentage of the number of cell nuclei in the same tissue size in control tissue.

Statistical analysis

Results are expressed as means ± SEM. Statistical analyses were performed by using the analysis of variance followed by Dunnett's multiple comparison *post hoc* test. Values of $p < 0.05$ were considered significant. To assess interobserver agreement, in case of histological evaluations, weighted kappa values were calculated.

Acknowledgments

This study was supported by National Development Agency grants (TÁMOP-4.2.2-08/1/2008-0002 and 0013; TÁMOP-4.2.1.B-09/1/KONV-2010-0005), the Hungarian Scientific Research Fund (K78311 to Z.R., NNF 78851 to P.H., and PD78087 to V.V.), the Hungarian Academy of Sciences (BO 00334/08/5 to P.H. and BO 00174/10/5 to Z.R.), and the Academy of Finland (130087 to L.A.). The authors would like to thank Dr. Gizella Karácsony for her help with the TUNEL assay. The rabbit anti-HSP72 antibody was a generous gift from Dr. István Kurucz.

Author Disclosure Statement

No competing financial interests exist.

References

1. Bernacki RJ, Bergeron RJ, and Porter CW. N,N′-bis(ethyl)spermine homologues against human MALME-3 melanoma xenografts. *Cancer Res* 52: 2424–2430, 1992.
2. Bradford MM. A rapid and sensitive method for the quantitation of microgram quantities of protein utilizing the principle of protein-dye binding. *Anal Biochem* 72: 248–254, 1976.
3. Bohus E, Coen M, Keun HC, Ebbels TM, Beckonert O, Lindon JC, Holmes E, Noszál B, and Nicholson JK. Temporal metabonomic modeling of l-arginine-induced exocrine pancreatitis. *J Proteome Res* 7: 4435–4445, 2008.
4. Chiu DT, Stults FH, and Tappel AL. Purification and properties of rat lung soluble glutathione peroxidase. *Biochim Biophys Acta* 445: 558–566, 1976.
5. Czakó L, Takács T, Varga IS, Tiszlavicz L, Hai DQ, Hegyi P, Matkovics B, and Lonovics J. Involvement of oxygen-derived free radicals in L-arginine-induced acute pancreatitis. *Dig Dis Sci* 43: 1770–1777, 1998.
6. Dawra R, Sherif R, Phillips PA, Dudeja V, Dhaulakhandi D, and Saluja AK. Development of a new mouse model of acute pancreatitis induced by administration of L-arginine. *Am J Physiol Gastrointest Liver Physiol* 292: G1009–G1018, 2007.
7. Fang S, Thomas RM, Conklin JL, Oberley LW, and Christensen J. Co-localization of manganese superoxide dismutase and NADH diaphorase. *J Histochem Cytochem* 43: 849–855, 1995.
8. Gukovskaya AS, Gukovsky I, Jung Y, Mouria M, and Pandol SJ. Cholecystokinin induces caspase activation and mitochondrial dysfunction in pancreatic acinar cells. Roles in cell injury processes of pancreatitis. *J Biol Chem* 277: 22595–22604, 2002.
9. Gukovsky I, Gukovskaya AS, Blinman TA, Zaninovic V, and Pandol SJ. Early NF-kappaB activation is associated with hormone-induced pancreatitis. *Am J Physiol* 275: G1402–G1414, 1998.
10. Hegyi P, Rakonczay Z, Jr., Sári R, Góg C, Lonovics J, Takács T, and Czakó L. L-arginine-induced experimental pancreatitis. *World J Gastroenterol* 10: 2003–2009, 2004.
11. Hofbauer B, Saluja AK, Lerch MM, Bhagat L, Bhatia M, Lee HS, Frossard JL, Adler G, and Steer ML. Intra-acinar cell activation of trypsinogen during caerulein-induced pancreatitis in rats. *Am J Physiol Gastrointest Liver Physiol* 275: G352–G362, 1998.
12. Hyvönen T, Keinänen TA, Khomutov AR, Khomutov RM, and Eloranta TO. Monitoring of the uptake and metabolism of aminooxy analogues of polyamines in cultured cells by high-performance liquid chromatography. *J Chromatogr* 574: 17–21, 1992.
13. Hyvönen MT, Herzig KH, Sinervirta R, Albrecht E, Nordback I, Sand J, Keinänen TA, Vepsäläinen J, Grigorenko N, Khomutov AR, Krüger B, Jänne J, and Alhonen L. Activated polyamine catabolism in acute pancreatitis: alpha-methylated polyamine analogues prevent trypsinogen activation and pancreatitis-associated mortality. *Am J Pathol* 168: 115–122, 2006.
14. Kishino Y, Takama S, and Kitajima S. Ultracytochemistry of pancreatic damage induced by excess lysine. *Virchows Arch B Cell Pathol Incl Mol Pathol* 52: 153–167, 1986.
15. Kitajima S and Kishino Y. Pancreatic damage produced by injecting excess lysine in rats. *Virchows Arch B Cell Pathol Incl Mol Pathol* 49: 295–305, 1985.
16. Kubisch CH, Sans MD, Arumugam T, Ernst SA, Williams JA, and Logsdon CD. Early activation of endoplasmic reticulum stress is associated with arginine-induced acute pancreatitis. *Am J Physiol Gastrointest Liver Physiol* 291: G238–G245, 2006.
17. Kuebler WM, Abels C, Schuerer L, and Goetz AE. Measurement of neutrophil content in brain and lung tissue by a modified myeloperoxidase assay. *Int J Microcirc Clin Exp* 16: 89–97, 1996.
18. Kurucz I, Tombor B, Prechl J, Erdö F, Hegedűs E, Nagy Z, Vitai M, Korányi L, and László L. Ultastructural localization of HSP-72 examined with a new polyclonal antibody raised against the truncated variable domain of the heat shock protein. *Cell Stress Chaperones* 4: 139–152, 1999.
19. Laemmli UK. Cleavage of structural proteins during the assembly of the head of bacteriophage T4. *Nature* 227: 680–685, 1970.
20. Matkovics B, Novák R, and Szőllősi I. Peroxide anyagcsere enzimek; szuperoxid dizmutáz; peroxidaz és kataláz meghatározása laboratóriumi anyagokban. *Lab Diagnosztika* 4: 91–94, 1977.
21. Misra HP and Fridovich I. The role of superoxide anion in the autoxidation of epinephrine and a simple assay for superoxide dismutase. *J Biol Chem* 247: 3170–3175, 1972.
22. Odinokova IV, Sung KF, Mareninova OA, Hermann K, Gukovsky I, and Gukovskaya AS. Mitochondrial mechanisms of death responses in pancreatitis. *J Gastroenterol Hepatol* 23 Suppl 1: S25–S30, 2008.
23. Odinokova IV, Sung KF, Mareninova OA, Hermann K, Evtodienko Y, Andreyev A, Gukovsky I, and Gukovskaya AS. Mechanisms regulating cytochrome c release in pancreatic mitochondria. *Gut* 58: 431–442, 2009.
24. Pandol SJ, Saluja AK, Imrie CW, and Banks PA. Acute pancreatitis: bench to the bedside. *Gastroenterology* 132: 1127–1151, 2007.
25. Petersen OH, Tepikin AV, Gerasimenko JV, Gerasimenko OV, Sutton R, and Criddle DN. Fatty acids, alcohol and fatty acid ethyl esters: toxic Ca2+ signal generation and pancreatitis. *Cell Calcium* 45: 634–642, 2009.
26. Rakonczay Z, Jr., Jármay K, Kaszaki J, Mándi Y, Duda E, Hegyi P, Boros I, Lonovics J, and Takács T. NF-κB activation is detrimental in arginine-induced acute pancreatitis. *Free Radic Biol Med* 34: 696–709, 2003.
27. Rakonczay Z, Jr., Hegyi P, Takács T, McCarrol J, and Saluja AK. The role of NF-κB activation in the pathogenesis of acute pancreatitis. *Gut* 57: 259–267, 2008.
28. Rakonczay Z, Jr., Hegyi P, Dósa S, Iványi B, Jármay K, Biczó G, Hracskó Z, Varga IS, Karg E, Kaszaki J, Varró A, Lonovics J, Boros I, Gukovsky I, Gukovskaya AS, Pandol SJ, and Takács T. A new severe acute necrotizing pancreatitis model induced by L-ornithine in rats. *Crit Care Med* 36: 2117–2127, 2008.

29. Saluja AK, Donovan EA, Yamanaka K, Yamaguchi Y, Hofbauer B, and Steer ML. Cerulein-induced *in vitro* activation of trypsinogen in rat pancreatic acini is mediated by cathepsin B. *Gastroenterology* 113: 304–310, 1997.
30. Sedlak J and Lindsay RH. Estimation of total, protein-bound and non-protein sulfhydryl group in tissue with Ellman's reagent. *Anal Biochem* 25: 192–205, 1998.
31. Tani S, Itoh H, Okabayashi Y, Nakamura T, Fujii M, Fujisawa T, Koide M, and Otsuki M. New model of acute necrotizing pancreatitis induced by excessive doses of arginine in rats. *Dig Dis Sci* 35: 367–374, 1990.

Address correspondence to:
Dr. Zoltán Rakonczay
First Department of Medicine
University of Szeged
P.O. Box: 427
H-6701 Szeged
Hungary

E-mail: raz@in1st.szote.u-szeged.hu

Date of first submission to ARS Central, May 12, 2011; date of acceptance, June 6, 2011.

Abbreviations Used

$\Delta\Psi m$ = mitochondrial membrane potential
ADP = adenosine diphosphate
ASAT = aspartate amino transferase
ATP = adenosine triphosphate
DNP = dinitrophenol
GSH-Px = glutathione peroxidase
HSP72 = heat-shock protein 72
IL-1β = interleukin-1β
i.p. = intraperitoneal(ly)
MPO = myeloperoxidase
mPTP = mitochondrial permeability transition pore
NF-κB = nuclear factor-κB
NSG = nonprotein sulfhydryl group
PS = physiological saline
p.w./b.w. = pancreatic weight/body weight ratio
RLM = rat liver mitochondria
RPM = rat pancreatic mitochondria
SOD = superoxide dismutase
SSAT = spermidine/spermine N^1-acetyltransferase
TPP^+ = tetraphenyl phosphonium ion
TUNEL = TdT-mediated dUTP nick end-labeling

This article has been cited by:

1. Svetlana Voronina, Alexei Tepikin. 2012. Mitochondrial calcium in the life and death of exocrine secretory cells. *Cell Calcium* **52**:1, 86-92. [CrossRef]
2. Ilya Gukovsky, Stephen J Pandol, Olga A Mareninova, Natalia Shalbueva, Wenzhuo Jia, Anna S Gukovskaya. 2012. Impaired autophagy and organellar dysfunction in pancreatitis. *Journal of Gastroenterology and Hepatology* **27**, 27-32. [CrossRef]